Amyloid Oligomer Formation Probed by Water Proton Magnetic Resonance Spectroscopy

J. H. Walton,[†] R. S. Berry,[‡] and F. Despa[§*]
[†]NMR Facility and Biomedical Engineering Graduate Group, University of California, Davis, California; [‡]Department of Chemistry and James Franck Institute, The University of Chicago, Chicago, Illinois; and [§]Department of Pharmacology, University of California, Davis, California

ABSTRACT Formation of amyloid oligomers, the most toxic species of amyloids in degenerative diseases, is critically coupled to the interplay with surrounding water. The hydrophobic force driving the oligomerization causes water removal from interfaces, changing the surface-hydration properties. Here, we show that such effects alter the magnetic relaxation response of local water in ways that may enable oligomer detection. By using water proton magnetic resonance spectroscopy, we measured significantly longer transverse magnetic relaxation (T_2) times in mixtures of serum and amyloidogenic A$\beta_{1\text{-}42}$ peptides versus similar concentration solutions of serum and nonamyloidogenic scrambled A$\beta_{42\text{-}1}$ peptides. Immunochemistry with oligomer-specific antibodies, electron microscopy and computer simulations demonstrated that the hyperintense magnetic signal correlates with A$\beta_{1\text{-}42}$ oligomerization. Finding early biophysical markers of the oligomerization process is crucial for guiding the development of new noninvasive imaging techniques, enabling timely diagnosis of amyloid-related diseases and pharmacological intervention.

INTRODUCTION

Amyloids are proteinaceous fibrils that can be derived by the aggregation of a large variety of proteins (1). Accumulation of amyloids in susceptible tissues represents the common manifestation of many degenerative diseases (2,3). Well-known examples (1–4) include deposition of Aβ fibrillar plaques in the brains of Alzheimer's disease (AD) patients, accumulation of islet amyloid polypeptide (IAPP) fibrils in pancreatic islets of type-2 diabetics, and formation of serum protein transthyretin deposits in cardiac tissues (the hallmark of heart amyloidoses).

There is emerging clinical and experimental evidence (5,6) suggesting that the occurrence of amyloid deposits could actually be a defense mechanism used to avoid serious tissue degradation whereas the major toxic effects to cells are mediated by soluble amyloid oligomers. Data collected from various human pathological tissues, including AD brain (7), diabetic pancreatic islets (8), and failing hearts (9,10), show that soluble amyloid oligomers are distinct, spatially segregated molecular entities. They presumably attach to cellular membranes, inducing cell dysfunction and apoptosis (8), or aggregate-forming fibril bundles (7). Early detection of amyloid oligomers is crucial for treating, inhibiting the progression, and preventing devastating effects of amyloid-related diseases.

The amyloid oligomer represents an amorphous molecular aggregate formed by the association of small numbers (tens or fewer) of amyloid monomers (11,12). Molecular-dynamics simulations in explicit solvent show that soluble oligomer species consist actually of various β-barrel structures in equilibrium with amorphous states and fibrillike assemblies (13). Immunochemistry with conformation-specific antibodies suggests that the occurrence of different preamyloid species is the result of competing reaction pathways that are thermodynamically distinct (14).

Temperature, concentration, and solvent conditions can have a strong impact on the structure and dynamics of these molecular species, in vitro (15,16). Formation and accumulation of amyloidogenic entities in vivo are more complex, because these entities are also potentially membrane-interacting (reviewed by Meredith (17)). From the point of view of aggregation, conditions that favor binding of the protein to membranes also disfavor formation of isolated fibrils, suggesting that these two processes are opposed to one another. Cell membranes can act indeed as sites of accumulation for amyloidogenic peptides (17), such as IAPP, favoring IAPP fibril growth at the membrane (18). On the other hand, recent studies revealed the presence of IAPP oligomers in secretory vesicles of pancreatic β-cells (8,19,20), blood, and heart tissues (10), suggesting that IAPP oligomers can travel through the circulation system as distinct entities.

Amyloid oligomer formation is critically coupled to the interplay with surrounding water. The force driving amyloid monomers to oligomerize is mostly hydrophobic in nature, causing water removal from interfaces and changing the surface-hydration properties. Thus, oligomerization can alter the bulklike/surface-water ratio and induce rearrangements of local solvent networks in ways that may enable oligomer detection. Previous studies suggested that surface hydration properties of proteins determine the microscopic magnetic relaxation response of surrounding water (21–24).

Recently, Nucci et al. (24) demonstrated that water proton magnetic resonance spectroscopy can resolve dynamics of water at the surface of proteins. Moreover, the results (24) suggest that water-rearrangement processes in the next hydration layers closely correlate with hydration properties of specific water patches on the protein surface (25), which

Submitted February 1, 2011, and accepted for publication March 25, 2011.

*Correspondence: fdespa@ucdavis.edu

Editor: Josh Wand.

0006-3495/11/05/2302/7 $2.00

doi: 10.1016/j.bpj.2011.03.029

was also predicted by computer simulations (22,26,27). The work by Nucci et al. (24) supports also the idea (21–23) that the magnetic relaxation of water in the hydration shells of proteins is a valuable tool to probe pathogenic proteins associated with many diseases.

Here, we investigate the magnetic relaxation response of water in mixtures of serum and amyloidogenic $A\beta_{1\text{-}42}$ peptides versus similar concentration solutions of serum and nonamyloidogenic scrambled $A\beta_{42\text{-}1}$ peptides by using water proton magnetic resonance spectroscopy (MRS). Immunochemistry with oligomer-specific antibodies, electron microscopy, and computer simulations are used to uncover the most likely amyloid structures associated with the magnetic signal recorded in each protein mixture. This study may give a new impetus to the development of efficient experimental protocols for early detection of amyloid-related diseases.

MATERIALS AND METHODS

The key experimental factor in the water proton MRS approach used by Nucci et al. (24) is the encapsulation of proteins in small cages, e.g., in reverse micelles (28), to slow hydration dynamics and hydrogen-exchange kinetics of proteins. Increasing the fraction of local water protons with slower reorientations along the applied magnetic field compared with the ultrafast reorientation of bulklike water protons enables protein detection (25). Based on these facts, we assume that amyloid oligomer formation in a low viscosity fluid, e.g., serum, can alter significantly the fraction of bulklike/surface water to induce a distinct magnetic resonance signal.

The following basic question is being addressed. Assume a system of N background serum proteins in a given environment of volume V. Suppose we replace ΔN serum proteins with amyloidogenic $A\beta_{1\text{-}42}$ peptides. The amyloidogenic peptides associate, forming soluble amyloid oligomers and protofibrils. The $A\beta_{1\text{-}42}$ oligomerization process can alter bulklike/surface water, change surface-hydration properties, and induce rearrangements of local water networks. In contrast, the replacement of serum proteins by (the same amount of) nonamyloidogenic $A\beta_{42\text{-}1}$ isomers may not alter significantly dynamics of water molecules, because $A\beta_{42\text{-}1}$ does not oligomerize.

What is the relative change of water proton magnetic relaxation time (T_2) after morphological transitions from monomers to soluble amyloid species?

To answer this question, we combine experimental approaches, including water proton MRS, immunochemistry with oligomer-specific antibodies and electron microscopy (EM), and computer simulations.

Experimental

Amyloidogenic $A\beta_{1\text{-}42}$

DAEFRHDSGYEVHHQKLVFFAED

VGSNKGAIIGLMVGGVVIA

and $A\beta_{42\text{-}1}$

AIAEGDSHVLKEGAYMEIFDVQGH

VFGGKIFRVVDLGSHNVA

scrambled isoforms are test peptides (from Anaspec, Fremont, CA) in this study. As protein background, we used bovine serum, a biological medium containing mainly water (~90%) and bovine serum albumin proteins. Stock peptide solutions were mixed with bovine serum at final peptide concentrations of 5, 50, and 100 μM in a 0.7-mL volume. All protein solutions, i.e., mixtures of serum and amyloidogenic or nonamyloidogenic peptides or just serum, were prepared at the same volume (0.7 mL), pH, and temperature conditions. Sodium azide (0.02%) was added in solutions to prevent microbial growth. Protein solutions were incubated at room temperature for 3 h, without stirring, to allow the amyloidogenic peptides to associate and form oligomers and fibrils.

Prior measurements, protein solutions were transferred in 5-mm high-resolution NMR tubes. The proton transverse magnetic relaxation time (T_2) decay in each protein sample was measured at 3 h after starting the aggregation reaction and repeated next day (~24 h). The measurements were done with a 9.4 T MR scanner (Oxford Instruments, Abingdon, Oxfordshire, UK) with an 89-mm-wide-bore magnet. To capture the essential characteristics of the magnetic relaxation response of the solvation water, we used a Carr-Purcell-Maiboom-Gill T_2 relaxation pulse sequence with a 1-ms echo spacing and an echo train length of 1 s. T_2 decay curves were analyzed with a nonnegative least-squares algorithm to derive the characteristic T_2 time of the magnetic signal (29).

To uncover the most likely amyloidogenic entities associated with the T_2-MR signal in each protein solution, we carried out dot-blot assays using conformation-dependent antibodies. Immunochemistry tests with conformation-dependent antibodies provide direct evidence for oligomer and fibril formation (7,14). The anti-oligomer-specific antibody A11 recognizes the nonfibrillar oligomeric conformation, but not the monomer or the fibrillar oligomeric structures (7–9,14). Conversely, the anti-fibril-specific antibody OC recognizes the fibrillar oligomers (protofibrils), but not nonfibrillar oligomers or monomers (14). The dot-blot assay is a technique for detecting, analyzing, and identifying proteins. Briefly, 2-μL aliquots of each oligomerization reaction are applied onto nitrocellulose membranes. The membranes are blocked for 1 h at room temperature (RT) or overnight at 4°C with 10% nonfat milk in Tris-buffered saline containing 0.01% TWEEN 20. (TWEEN 20 is a detergent used for solubilizing proteins.)

The membranes are then washed in 0.01% TWEEN 20 and incubated with affinity-purified conformation-dependent antibodies for 1–2 h at RT. Membranes are washed again and incubated with a secondary antibody (horseradish peroxidase-conjugated) for 1 h (RT). Then, the membranes are washed and developed with an electrochemiluminescence kit. Data were collected at the initial time point (3 h) as for the T_2-MR measurement and, afterwards, repeated daily for up to three days, to monitor morphological changes in the protein solutions. For assessing the clumps of amyloid fibrils and amyloid deposition, we measured the Thioflavin T (ThT) fluorescence in amyloidogenic protein samples at three days after starting the oligomerization reactions. For measurements in solutions, we used a microplate-reader fluorometer with excitation at 458 nm (Ar laser) and fluorescence collected at >475 nm. The fluorescence intensity was corrected for background and normalized using the baseline serum fluorescence level.

To visualize the nature of molecular entities formed in solutions, aliquots of each aggregation reaction were imaged by a CM 12 electron microscope (Philips Electron Optics, FEI, Hillsboro, OR) at the same time points as for dot blot and water proton MRS measurements. Electron microscopy (EM) images were taken also at the end point of the oligomerization process to visualize amyloid deposition. Specimen preparation followed the procedure described in the article of Paravastu et al. (30). Clumping of protofibrils and amyloid fibril deposition in solutions were also assessed also by ThT fluorescence by using a microplate-reader fluorometer, with excitation at 450 nm and emission at 482 nm.

Theoretical

The characteristic relaxation rate of water depends on the motion of water molecules through the spectral density function. The spectral density function is usually approximated by the Lorentzian

$$J(\omega,\ \tau) \sim \frac{\tau}{1+(\omega\,\tau)^2},$$

where ω is the frequency of the applied field and τ represents the rotational relaxation time of water molecules in the local environment. Because the oligomerization process alters significantly the surface/bulk water, we considered here two main water pools in each protein system, surface (X_s) and bulk-like (X_b) waters. The characteristic rotational relaxation times for surface and bulk water molecules are approximated by $\tau_S \cong 10^{-10}$ s and $\tau_b \cong 10^{-12}$ s (22,28), respectively.

Normally, the recorded signal is a superposition of the relaxation responses from these two water phases (22,28):

$$\frac{1}{T_2} = X_S\,C\,[3\,\tau_S + 5\,J(\omega_L,\ \tau_S) + 2\,J(2\,\omega_L,\ \tau_S)] + X_b\,C\,[3\,\tau_b + 5\,J(\omega_L,\ \tau_b) + 2\,J(2\,\omega_L,\ \tau_b)]. \quad (1)$$

Here, C stands for the strength of the magnetic dipole-dipole coupling ($C \cong 8\ 10^9\ s^{-2}$) and ω_L represents the Larmor frequency of the water protons in the magnetic field of the MR scanner. The Larmor frequency depends on the intensity of the magnetic field (B_0) and proton gyromagnetic ratio ($\gamma = 2.67510^8\ s^{-1}\ T^{-1}$), $\omega_L = \gamma\,B_0$, where $B_0 = 9.4\ T$.

Water molecules at the interface with amyloidogenic peptides undergo considerable reorganization during the aggregation process (11,12,21–23,31,32). As the peptides associate forming oligomers and fibrils, their hydrophobic patches are buried inside the newly formed amyloidogenic assembly. This gradually liberates more water molecules into the bulklike water phase, decreasing the fraction of water molecules in direct contact with the molecular surface (21–23). Based on the scaled particle theory (33), we can estimate the amount (ΔV) of surface water released in the bulk after the oligomerization process.

According to this theory, the intrinsic volume (V_m) of a macromolecule plus a shell of thickness l which results from the mutual thermal motions of the macromolecule and neighbor water molecules form the partial volume V^0, $V^0 \cong V_m + asa\ l$, where asa represents the water-accessible surface area of the monomer. V^0 is roughly $1.11\ V_m$ (22), so the thickness of the hydration shell can be approximated by

$$l \cong 0.11\frac{V_m}{asa}$$

and the volume of water at the macromolecular surface becomes $V_s \cong 0.11\ V_m$. The amount of water in the hydration shells of the amyloidogenic proteins is roughly equal to $\Delta N\ 0.11\ V_m$. Let us now assume that all ΔN amyloidogenic proteins clustered together, forming an aggregate with the water-accessible surface area ASA. Although the total amount of surface water of the newly formed molecular structure may depend on the structural morphology, the thickness (l) of the hydration shell remains in the same range as for individual peptides,

$$l \cong 0.11\frac{V_m}{asa}.$$

Therefore, we can approximate the amount of water in the surface layer of this molecular composite by

$$V_s^* \cong 0.11\,\frac{ASA}{asa}\,V_m.$$

For simplicity, we can consider that

$$\frac{ASA}{asa}$$

scales with $(\Delta N)^{2/3}$, hence the volume of water confined at the surface of the composite can be written as

$$V_s^* \cong 0.11\ (\Delta N)^{2/3} V_m.$$

Therefore, the fraction $\Delta X = \Delta V/V$ of water released in the bulk after the aggregation of ΔN amyloidogenic is given by

$$\Delta X \cong \frac{0.11\ \Delta N V_m - 0.11\ (\Delta N)^{2/3} V_m}{V}. \quad (2)$$

Obviously, the fraction of surface water corresponding to an amyloidogenic protein system in oligomeric form is significantly smaller than that corresponding to the same system in which the amyloidogenic peptides are in monomeric forms. The relative change of surface and bulklike water fractions $X_S \rightarrow X_S - \Delta X$ and $X_b \rightarrow X_b - \Delta X$ rescale the transverse magnetic relaxation time $T_2 \rightarrow T_2 + \Delta T_2$. By using Eqs. 1 and 2, we can readily express the relative change of the magnetic relaxation time $\Delta T_2/T_2$ in terms of the initial T_2, when all proteins were in monomeric forms, and ΔX by

$$\frac{\Delta T_2}{T_2} \cong \Delta X\,C\,[3\,\tau_S + 5\,J(\omega_L,\ \tau_S) + 2\,J(2\,\omega_L,\ \tau_S) - 3\,\tau_b - 5\,J(\omega_L,\ \tau_b) - 2\,J(2\,\omega_L,\ \tau_b)]T_2. \quad (3)$$

RESULTS

Water proton T_2 was derived from the characteristic MR signal decay curve of each amyloidogenic/nonamyloidogenic peptide system. T_2 is in the time domain measured typically in serum, i.e., hundreds of milliseconds (Table 1). However, the replacement of background serum proteins with amyloidogenic A$\beta_{1\text{-}42}$ (Aβ) peptides increased significantly the T_2 of the surrounding water. In contrast, similar amounts of nonamyloidogenic scrambled A$\beta_{42\text{-}1}$ (AβS) peptides in serum induced no detectable T_2 change. At the

TABLE 1 T_2 magnetic relaxation times in mixtures of amyloidogenic Aβ peptides and serum versus same concentration solutions of nonamyloidogenic AβS in serum (experimental and computational data)

Peptide concentration in serum	Solutions		Water T_2 (exp.)	T_2 (theoretical)
100 μM Aβ	311 μL stock Aβ	389 μL serum	363 ± 7 ms	374 ms
100 μM AβS	311 μL stock AβS	389 μL serum	200 ± 1 ms	
50 μM Aβ	155 μL stock Aβ	545 μL serum	317 ± 7 ms	321 ms
50 μM AβS	155 μL stock AβS	545 μL serum	200 ± 1 ms	
5 μM Aβ	16 μL stock Aβ	684 μL serum	205 ± 7 ms	208 ms
5 μM AβS	16 μL stock AβS	684 μL serum	193 ± 7 ms	
	700 μL serum		200 ± 1 ms	

Baseline T_2 time in the theoretical approach was set to 200 ms (serum).

same sample volume (0.7 mL), pH, and temperature conditions, significant changes of water proton T_2 were observed starting from 2% volume fraction of stock Aβ peptide solution (Table 1).

Longer T_2 of water correlates with amyloid oligomer formation

In Fig. 1 *a*, we display the increase (ΔT_2) of the transverse magnetic relaxation time induced by the replacement of serum proteins with amyloidogenic Aβ peptides versus same amounts of nonamyloidogenic AβS isomers. ΔT_2 is significantly larger at higher Aβ volume fractions. Intriguingly, measured T_2-MR signal remained nearly constant in all protein mixtures for >24 h of incubation at room temperature, as we can see in Fig. 1 *b*.

To uncover the most likely amyloid species associated with the T_2 signal in each protein solution, we carried out dot blot assays using conformation-dependent antibodies (7,14). Aliquots were removed at various time points, spotted onto nitrocellulose membranes, and probed with A11 and OC conformation-specific antibodies. The aggregation process developed time-dependent immunoreactivity that became strongly visible after ~3 h, indicative of the oligomerization process (Fig. 1 *c*). The intensity of each dot in Fig. 1 *c* reflects the amount of nonfibrillar oligomers (*left-hand group*) and fibrillar structures (*right-hand group*) present in each reaction mixture. The mixtures contain heterogeneous populations of soluble amorphous and fibrillar oligomers, suggesting that these amyloid species are distinct and competing pathways (11).

Population densities of soluble oligomers and protofibrils increase with peptide concentration. The immunoreactivity signal remained fairly stable for up to three days. After three days of incubation at RT, we measured slightly decreased A11 (amorphous) and OC (fibril) specific immunoreactivities that can be attributed to the weakened binding of the amyloidogenic molecular entities to the nitrocellulose membranes caused by increased clumping and amyloid deposition. The relatively low kinetics of the conversion of amyloid monomers into fibrils and fibrillar clumps may be due to the presence of serum proteins that act as a buffer, lowering the cross-section area of the Aβ-Aβ intermolecular interactions. Clumping of protofibrils and amyloid fibril deposition in solutions were assessed by ThT fluorescence (see Fig. 1 *d*) and EM imaging (Fig. 2 *b*).

To visualize the nature of the molecular entities formed in solutions, aliquots of each aggregation reaction were imaged by transmission EM at the same time points as for dot blots and water proton T_2-MR measurements. Consistent with the immunochemistry tests, protein mixtures containing large amounts (100 μM) of amyloid peptides exhibited considerable aggregation reactions at ~24 h of incubation time. Specifically, the EM images (Fig. 2 *a*) show large amounts of amorphous aggregates (indicated by *bars*), i.e., nonfibrillar oligomers, and early forms of

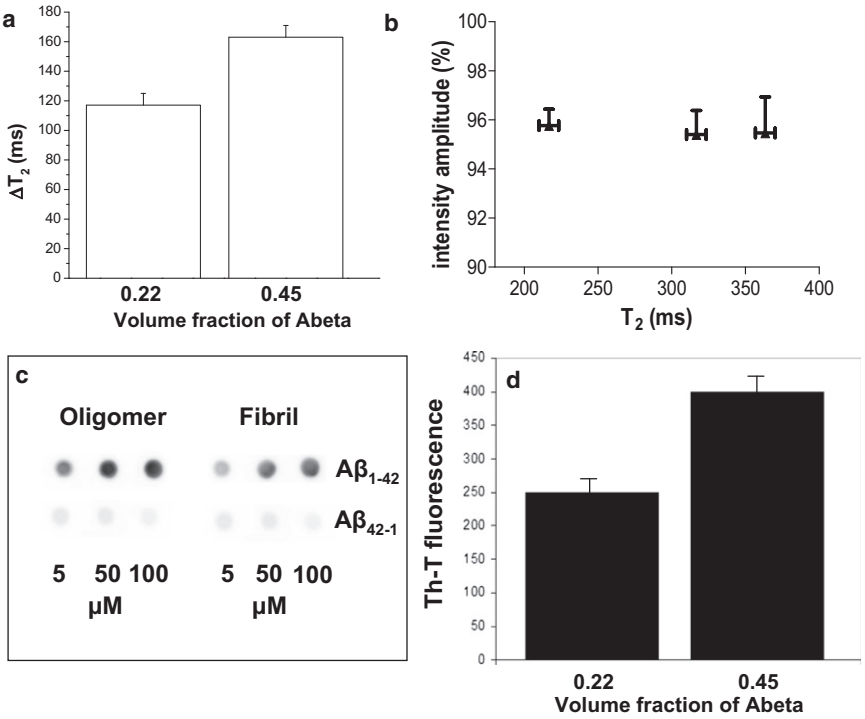

FIGURE 1 (*a*) Increase ΔT_2 of transverse magnetic relaxation time in A$\beta_{1\text{-}42}$ amyloidogenic protein systems relative to the magnetic signal in mixtures of serum and nonamyloidogenic isoform A$\beta_{42\text{-}1}$. The value ΔT_2 is significantly larger in serum mixtures containing increased concentrations of amyloidogenic peptides, a consequence of a much faster oligomerization process. (*b*) Mean signal intensity amplitudes and T_2 magnetic relaxation times (and characteristic standard errors) corresponding to water protons in Aβ-serum mixtures. Data are averages of the initial measurements, i.e., 3 h incubation time, and measurements at 24 h incubation time. The relative variation of the MR signal indicates that the formation of preamyloid species is a dynamic process in which the oligomers frequently undergo structural transitions. (*c*) Nonfibrillar oligomer-specific reactivity (*left-hand group*) and fibrillar oligomer-specific reactivity (*right-hand group*) from dot-blot assays using conformation-dependent antibodies. The anti-oligomer-specific antibody A11 recognizes the oligomeric conformation and not the monomer or the incipient fibrillar structure. Conversely, the anti-fibril-specific antibody OC recognizes the fibril, but not fibrillar oligomers or monomers. The intensity of each dot reflects the amount of fibrillar and nonfibrillar oligomers present in each reaction mixture. This increases with the peptide concentration. Aβ-serum mixtures contain heterogeneous populations of nonfibrillar and fibrillar preamyloid species. (*d*) ThT fluorescence revealing fibril formation in Aβ-serum mixtures. The fibril formation was assessed three days after the Aβ-serum incubation at RT.

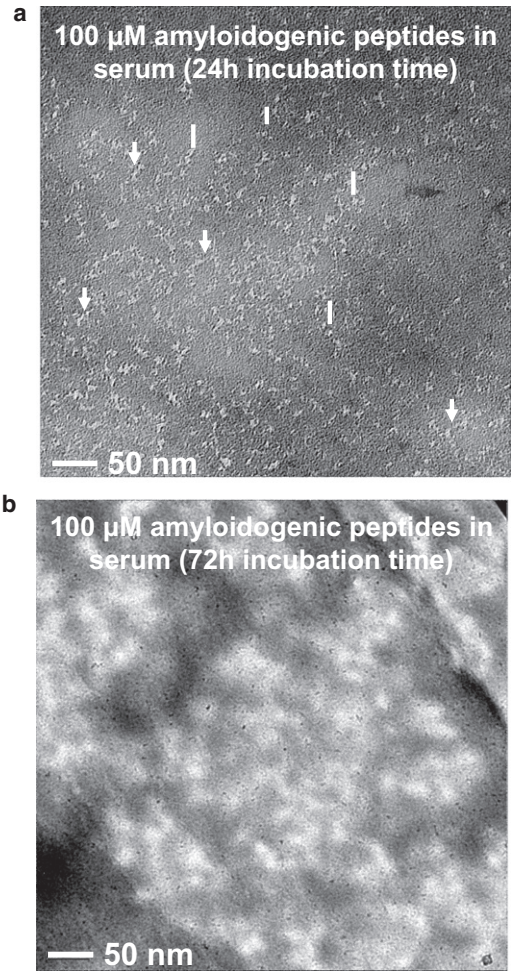

FIGURE 2 (*a*) Representative transmission EM image of Aβ-serum mixtures. Consistent with the immunochemistry tests, protein mixtures containing large amounts (100 μM) of amyloid monomers exhibited considerable aggregation reactions at ~24 h of incubation time. We can see early forms of elongated oligomers, i.e., protofibrils (*arrows*) and spheroidal structures of amorphous amyloid oligomers (*bars*). (*b*) Representative transmission EM image of Aβ-serum mixtures, three days after incubation at RT. Aβ formed large amyloid structures. Background serum proteins are most likely involved in Aβ fibril formation and deposition. This can be noted from the shapes of protein aggregates that are different from common fibrillar structures of homogeneous Aβ aggregation reported previously (12), resembling more scattered fibrillar plaques observed in tissues (35–38).

elongated aggregates, i.e., protofibrils (indicated by *arrows*). At low concentrations, we were not able to discriminate clearly the amyloid aggregates on transmission EM images. After three days of incubation at room temperature, Aβ formed larger amyloid structures that deposited at the bottom of the NMR tubes. A representative EM image showing such amyloid species is displayed in Fig. 2 *b*. Background serum proteins are most likely involved in Aβ fibril formation and deposition. This can be noted from the shapes of protein aggregates in Fig. 2 *b*, which are different from common fibrillar structures of homogeneous Aβ aggregation reported previously (30), and resemble more the scattered plaques observed in tissues (34–38).

A$\beta_{1\text{-}42}$ oligomerization increases bulklike to surface/water ratio, inducing longer T_2

By using Eq. 2, we estimated the increase of bulklike/surface water fraction after Aβ oligomerization. For Aβ volume fractions used in the present experiments, we estimated

$$\Delta X \cong 0.5\% \ (5\ \mu\text{M A}\beta),$$

$$\Delta X \cong 4.5\% \ (50\ \mu\text{M A}\beta), \text{ and}$$

$$\Delta X \cong 6.5\% \ (100\ \mu\text{M A}\beta),$$

respectively. By using Eq. 3 and ΔX derived as shown in above, we estimated the increase ΔT_2 in amyloidogenic Aβ systems relative to T_2 measured in nonamyloidogenic AβS mixtures. Predicted ΔT_2 results are in excellent agreement with experimental T_2 data (see Table 1). Moreover, replacing ΔX volume fractions of serum with water (which would represent the increase of bulklike water phase after Aβ oligomerization), we measured an upward shift of T_2 (see Fig. 3) in the same range as T_2 times displayed in Table 1.

DISCUSSION

The role water molecules play in protein structure (39–42), function (39–41), and aggregation (11,12,21–23,31,32,43,44) is known to be extensive, yet has not been fully explored. The key experimental feature enabling the study of water-protein coupling by MRS is encapsulation of proteins in microscopic water pools (e.g., reverse micelles) to slow protein hydration dynamics and

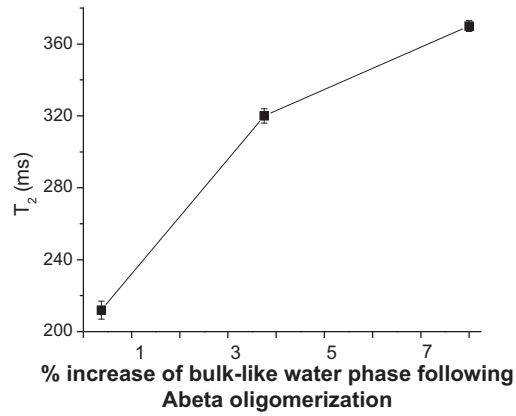

FIGURE 3 Experimental T_2 relaxation time of water protons after the replacement of ΔX = 0.5%, 4.5%, and 6.5% volume fraction of serum with water. ΔX represents the predicted increase of bulklike water phase after Aβ oligomerization (see Eq. 2). The upward shift of T_2 measured by MRS is in excellent agreement with theoretical predictions (see also Table 1).

hydrogen-exchange kinetics (24,25). Our data demonstrated that a matrix of serum provides an effective environment to study amyloid oligomer formation, which is also physiologically relevant. The presence of background serum proteins increases the fraction of slower water molecules at the surface of amyloid species, enabling detection.

Recent studies suggested that desolvation effects are critical to the formation and accumulation of amyloids (11,12,21–23). Our data show that the presence of amyloidogenic Aβ peptides in serum generates longer T_2 relaxation times of water compared to same concentration mixtures of serum and nonamyloidogenic AβS (Fig. 1 *a*). Immunochemistry with oligomer-specific antibodies (Fig. 1 *b*) and EM data (Fig. 2 *a*) demonstrated that longer T_2 correlates with $A\beta_{1\text{-}42}$ oligomerization. Our data support a molecular mechanism for the magnetic contrast of Aβ oligomer formation based on the restructuring of water at interfaces (Fig. 3, Table 1).

The relative increase of bulklike/surface-water shifts T_2 toward longer ($T_2 + \Delta T_2$) relaxation times, corresponding to bulklike water molecules (Fig. 3). Thus, the hyperintense magnetic signals of water in systems containing amyloidogenic proteins are early markers of the oligomerization process. This is the main result of our study. In principle, the approach could also discriminate between amyloid oligomers and fibrils, as we predicted previously (22,23). The amount of released water from interacting interfaces scales differently for amorphous oligomer versus fibril formation (22). However, measuring only ΔT_2 shift may not fully account for such changes. Rather, a plot T_2 versus peptide concentration may prove more relevant for this task.

In contrast to the incipient oligomerization and fibril formation, the association of amyloid fibrils in tangles and plaques (which may cage water between constituent fibrils (44)) is likely to induce hypo-intense MR responses, typical for structured (bound) water assemblies. MR images of amyloid samples display indeed both hypo- and hyperintense magnetic signals, i.e., dark and bright spots (34–38,45). The hypo-intense signal is commonly attributed to the iron present in amyloid plaques, which accelerates the magnetic relaxation of local water and increases the local MR contrast (5). Detection of individual oligomers by MR imaging is technically not feasible currently, due to an insufficient resolution of the MR imaging scanners (46).

This study shows that structural changes associated with oligomer formation have a unique impact on the overall proton MR signal reflected in the upward shift of the characteristic T_2 relaxation time of bulklike water. Thus, the presence of multiple, dynamically labile preamyloid structures in the environment may induce sizeable MR contrast to enable detection, if susceptible tissues for amyloid oligomer accumulation are identified sufficiently early. Immunofluorescence micrographs of AD human brain tissues clearly show closely packed preamyloid oligomers spreading on hundred-μm^2 size domains (7), which is normally accessible by MR imaging scanners (34–38).

Our results may give further impetus to the development of noninvasive techniques for identifying pathogenic proteins related to disease. For instance, water proton MRS tools and experimental protocols can be tuned to detect efficiently MR signal(s) of water molecules next to hydrophobic patches. This may prove extremely valuable in discriminating between toxic amyloid oligomers, which have an increased hydrophobic character (47), and other hydrophilic oligomers that have a lower propensity to attach to membranes and induce toxicity (47). Moreover, deciphering the magnetic relaxation response of water surrounding various embryonic amyloid species is important in fields as diverse as protein folding (39–42) and surface science (48,49).

The authors thank Professor C. Glabe of the University of California, Irvine, for providing the A11 and OC conformation-dependent antibodies used in this study.

The work was supported by the American Heart Association under grant No. 09BGIA2220165 (to F.D.) and by the Vision Grant from UC Davis Health System (to F.D.).

REFERENCES

1. Dobson, C. M. 2003. Protein folding and misfolding. *Nature.* 426:884–890.
2. Selkoe, D. J. 2003. Folding proteins in fatal ways. *Nature.* 426:900–904.
3. Chiti, F., and C. M. Dobson. 2006. Protein misfolding, functional amyloid, and human disease. *Annu. Rev. Biochem.* 75:333–366.
4. Westermark, P., C. Wernstedt, …, K. H. Johnson. 1987. Amyloid fibrils in human insulinoma and islets of Langerhans of the diabetic cat are derived from a neuropeptide-like protein also present in normal islet cells. *Proc. Natl. Acad. Sci. USA.* 84:3881–3885.
5. Benveniste, H., G. Einstein, …, G. A. Johnson. 1999. Detection of neuritic plaques in Alzheimer's disease by magnetic resonance microscopy. *Proc. Natl. Acad. Sci. USA.* 96:14079–14084.
6. Haass, C., and D. J. Selkoe. 2007. Soluble protein oligomers in neurodegeneration: lessons from the Alzheimer's amyloid β-peptide. *Nat. Rev. Mol. Cell Biol.* 8:101–112.
7. Kayed, R., E. Head, …, C. G. Glabe. 2003. Common structure of soluble amyloid oligomers implies common mechanism of pathogenesis. *Science.* 300:486–489.
8. Meier, J. J., R. Kayed, …, P. C. Butler. 2006. Inhibition of hIAPP fibril formation does not prevent β-cell death: evidence for distinct actions of oligomers and fibrils of hIAPP. *Am. J. Physiol.* 291:E1317–E1324.
9. Pattison, J. S., A. Sanbe, …, J. Robbins. 2008. Cardiomyocyte expression of a polyglutamine preamyloid oligomer causes heart failure. *Circulation.* 117:2743–2751.
10. Despa, S., L. Chen, …, F. Despa. 2009. Cardiac consequences of increased amylin secretion in diabetics. *Circulation.* 120:S457.
11. Schmit, J. D., K. Ghosh, and K. Dill. 2011. What drives amyloid molecules to assemble into oligomers and fibrils? *Biophys. J.* 100:450–458.
12. Petkova, A. T., R. D. Leapman, …, R. Tycko. 2005. Self-propagating, molecular-level polymorphism in Alzheimer's β-amyloid fibrils. *Science.* 307:262–265.
13. De Simone, A., and P. Derreumaux. 2010. Low molecular weight oligomers of amyloid peptides display β-barrel conformations: a replica exchange molecular dynamics study in explicit solvent. *J. Chem. Phys.* 132:165103.
14. Glabe, C. G. 2008. Structural classification of toxic amyloid oligomers. *J. Biol. Chem.* 283:29639–29643.

15. Ban, T., and Y. Goto. 2006. Direct observation of amyloid growth monitored by total internal reflection fluorescence microscopy. *Methods Enzymol.* 413:91–102.

16. Yagi, H., T. Ban, …, Y. Goto. 2007. Visualization and classification of amyloid β supramolecular assemblies. *Biochemistry.* 46:15009–15017.

17. Meredith, S. C. 2005. Protein denaturation and aggregation: cellular responses to denatured and aggregated proteins. *Ann. N. Y. Acad. Sci.* 1066:181–221.

18. Engel, M. F., L. Khemtémourian, …, J. W. Höppener. 2008. Membrane damage by human islet amyloid polypeptide through fibril growth at the membrane. *Proc. Natl. Acad. Sci. USA.* 105:6033–6038.

19. Despa, F. 2010. Endoplasmic reticulum overcrowding as a mechanism of β-cell dysfunction in diabetes. *Biophys. J.* 98:1641–1648.

20. Despa, F., and R. S. Berry. 2010. β-Cell dysfunction under hyperglycemic stress: a molecular model. *J. Diabetes Sci. Tech.* 4:1447–1456.

21. Despa, F., and R. S. Berry. 2007. The origin of long-range attraction between hydrophobes in water. *Biophys. J.* 92:373–378.

22. Despa, F., A. Fernández, …, R. S. Berry. 2008. Hydration profiles of amyloidogenic molecular structures. *J. Biol. Phys.* 34:577–590.

23. Despa, F. 2008. Bound water as a tool to detect soluble amyloid oligomers and amyloid protofibrils, the early stage of development of the Alzheimer's disease. *In* From Computational Biophysics to Systems Biology (CBSB08). NIC Series, *Vol. 36*. U. H. E. Hansmann, J. Meinke, S. Mohanty, W. Nadler, and O. Zimmermann, editors. Jülich, Germany. 193–196.

24. Nucci, N. V., M. S. Pometun, and A. J. Wand. 2011. Site-resolved measurement of water-protein interactions by solution NMR. *Nat. Struct. Mol. Biol.* 18:245–249.

25. Hilser, V. J. 2011. Structural biology: finding the wet spots. *Nature.* 469:166–167.

26. Virtanen, J. J., L. Makowski, …, K. F. Freed. 2010. Modeling the hydration layer around proteins: HyPred. *Biophys. J.* 99:1611–1619.

27. De Simone, A., G. G. Dodson, …, F. Fraternali. 2005. Prion and water: tight and dynamical hydration sites have a key role in structural stability. *Proc. Natl. Acad. Sci. USA.* 102:7535–7540.

28. Despa, F. 2008. Water confined in reverse micelles—probe tool in biomedical informatics. *Phys. Chem. Chem. Phys.* 10:4740–4747.

29. Stewart, W. A., A. L. MacKay, …, D. W. Paty. 1993. Spin-spin relaxation in experimental allergic encephalomyelitis. Analysis of CPMG data using a non-linear least squares method and linear inverse theory. *Magn. Reson. Med.* 29:767–775.

30. Paravastu, A. K., A. T. Petkova, and R. Tycko. 2006. Polymorphic fibril formation by residues 10–40 of the Alzheimer's β-amyloid peptide. *Biophys. J.* 90:4618–4629.

31. Meersman, F., and C. M. Dobson. 2006. Probing the pressure-temperature stability of amyloid fibrils provides new insights into their molecular properties. *Biochim. Biophys. Acta.* 1764:452–460.

32. Straub, J. E., and D. Thirumalai. 2010. Principles governing oligomer formation in amyloidogenic peptides. *Curr. Opin. Struct. Biol.* 20: 187–195.

33. Reiss, H. 1965. Scaled particle methods in the statistical thermodynamics of fluids. *Adv. Chem. Phys.* 9:1–84.

34. Lee, S. P., M. F. Falangola, …, J. A. Helpern. 2004. Visualization of β-amyloid plaques in a transgenic mouse model of Alzheimer's disease using MR microscopy without contrast reagents. *Magn. Reson. Med.* 52:538–544.

35. Reference deleted in proof.

36. Dhenain, M., N. Privat, …, R. E. Jacobs. 2002. Senile plaques do not induce susceptibility effects in T2*-weighted MR microscopic images. *NMR Biomed.* 15:197–203.

37. Jack, Jr., C. R., M. Garwood, …, J. F. Poduslo. 2004. In vivo visualization of Alzheimer's amyloid plaques by magnetic resonance imaging in transgenic mice without a contrast agent. *Magn. Reson. Med.* 52:1263–1271.

38. Jack, Jr., C. R., T. M. Wengenack, …, J. F. Poduslo. 2005. In vivo magnetic resonance microimaging of individual amyloid plaques in Alzheimer's transgenic mice. *J. Neurosci.* 25:10041–10048.

39. Frauenfelder, H., G. Chen, …, R. D. Young. 2009. A unified model of protein dynamics. *Proc. Natl. Acad. Sci. USA.* 106:5129–5134.

40. Levy, Y., and J. N. Onuchic. 2004. Water and proteins: a love-hate relationship. *Proc. Natl. Acad. Sci. USA.* 101:3325–3326.

41. Ebbinghaus, S., A. Dhar, …, M. Gruebele. 2010. Protein folding stability and dynamics imaged in a living cell. *Nat. Methods.* 7: 319–323.

42. Johnson, M. E., C. Malardier-Jugroot, and T. Head-Gordon. 2010. Effects of co-solvents on peptide hydration water structure and dynamics. *Phys. Chem. Chem. Phys.* 12:393–405.

43. Despa, F., A. Fernández, and R. S. Berry. 2004. Dielectric modulation of biological water. *Phys. Rev. Lett.* 93:228104.

44. Nelson, R., M. R. Sawaya, …, D. Eisenberg. 2005. Structure of the cross-β spine of amyloid-like fibrils. *Nature.* 435:773–778.

45. Vanhoutte, G., I. Dewachter, …, A. Van der Linden. 2005. Noninvasive in vivo MRI detection of neuritic plaques associated with iron in APP [V717I] transgenic mice, a model for Alzheimer's disease. *Magn. Reson. Med.* 53:607–613.

46. Tyszka, J. M., S. E. Fraser, and R. E. Jacobs. 2005. Magnetic resonance microscopy: recent advances and applications. *Curr. Opin. Biotechnol.* 16:93–99.

47. Campioni, S., B. Mannini, …, F. Chiti. 2010. A causative link between the structure of aberrant protein oligomers and their toxicity. *Nat. Chem. Biol.* 6:140–147.

48. Moilanen, D. E., E. E. Fenn, …, M. D. Fayer. 2009. Geometry and nanolength scales versus interface interactions: water dynamics in AOT lamellar structures and reverse micelles. *J. Am. Chem. Soc.* 131:8318–8328.

49. Granick, S., and S. C. Bae. 2008. Chemistry. A curious antipathy for water. *Science.* 322:1477–1478.